

The Hydrogen Bond of the One-Dimensional Assembled Complex $[\text{Ni}(\text{2,2'}$ -biimidazole) $]\text{2}$: The Effect of Transition Metals on the Hydrogen Bond

Hirotohi Mori and Eisaku Miyoshi*

Graduate School of Engineering Sciences, Kyushu University, 6-1 Kasuga Park, Fukuoka 816-8580

Received September 24, 2003; E-mail: miyoshi@asem.kyushu-u.ac.jp

The topologies of hydrogen-bond potential energy surfaces of one-dimensional assembled 2,2'-biimidazole (H_2bim) and its deprotonated Ni complex ($[\text{Ni}^{\text{II}}(\text{Hbim})_2]$) were investigated by density functional theory calculations at the B3LYP/CEP-31G(d,p) level. It was revealed that the formation of coordination bonds between Hbim and Ni makes the N–H...N hydrogen bond between Hbim units linear and strong.

The construction of molecular crystals formed from self-organization is one of the most important methods for developing new functional materials.^{1,2} It is well known that weak interactions, such as hydrogen-bonding interactions or π – π dispersion interactions, play an important role in constructing self-organized structures in many biological systems. Thus, to investigate model compounds with such weak interactions is a useful way to examine new functional materials.

Recently, Tadokoro et al. synthesized self-organizing metal complexes by using transition metals and 2,2'-biimidazolate mono-anions (Hbim^-).^{1,2} Hbim^- is one of the difunctional bridging ligands that forms not only a stable transition-metal (TM)-chelate complex, but also intermolecular hydrogen bonds with two sets of NH donors and N acceptors, as shown in Fig. 1(a). They used several transition metals (TM = Co, Ni, Cu, Ru) and succeeded to create 1-dimensional, 2-dimensional, and 3-dimensional regular crystal structures.² Their experimental results imply that the TMs in these complexes strengthen the intermolecular hydrogen-bonding interaction to form assembled complexes. Because the hydrogen bonds in these com-

plexes have a symmetric structure, the hydrogen-bond potential energy surface (PES) becomes double-minimum, as shown in Fig. 2. Unfortunately, however, no information regarding the strength of the intermolecular hydrogen-bonding interaction and the PES in these TM complexes was obtained from their experimental results.

The purpose of the present work is to clarify the effect of TMs on intermolecular hydrogen-bonding interactions to form an assembled complex, $[\text{TM}(\text{Hbim})_2]$. To investigate the hydrogen-bonding PESs of $[\text{TM}(\text{Hbim})_2]$ is very important for creating new functional materials, because the PESs contain key information regarding the nature of functional materials. As a first step in this direction, we investigated in the present study the PESs of $[\{\text{Ni}^{\text{II}}(\text{Hbim})_2\}_n]$ compared with those of $(\text{H}_2\text{bim})_n$ (see Fig. 1(b)) with $n = 2$ –4.

Computational Details

The present study deals with the topology of the hydrogen-bond PESs of the H_2bim and Hbim^- one-dimensional assembled transition-metal complexes. The electronic structures of these systems were obtained by density functional theory (DFT) calculations with the B3LYP hybrid functional. Although DFT calculations are generally suitable for studying the electronic structures of transition-metal complexes, they sometimes fail to describe intermolecular interactions. To examine the intermolecular interaction picture of DFT calculations, MP2 calculations at the B3LYP optimized point (MP2//B3LYP) were also performed. The basis sets used in above-mentioned calculations were CEP-31G augmented with a set of (d,p) type polarization functions (exponents d:0.80, p:1.10). All of the core electrons in the heavy atoms were replaced by the SBKJC effective core potentials (ECPs).^{3,4}

We recently investigated relativistic correlating basis sets for the main-group elements, and found that nodeless-type ECPs, such as SBKJC, have an inclination to overestimate the correlation energies, recommending the use of the ECP methods, which can produce valence orbitals with nodal structures.⁵ The model core potential (MCP) method⁶ is capable of produc-

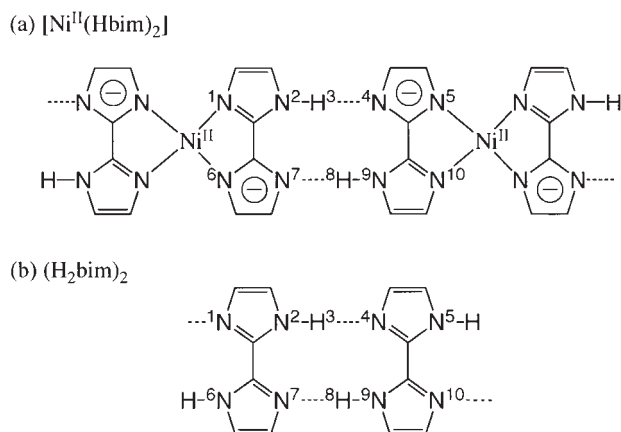


Fig. 1. Geometries of one-dimensional complexes (a) $[\{\text{Ni}(\text{Hbim})_2\}_n]$ and (b) $(\text{H}_2\text{bim})_n$.

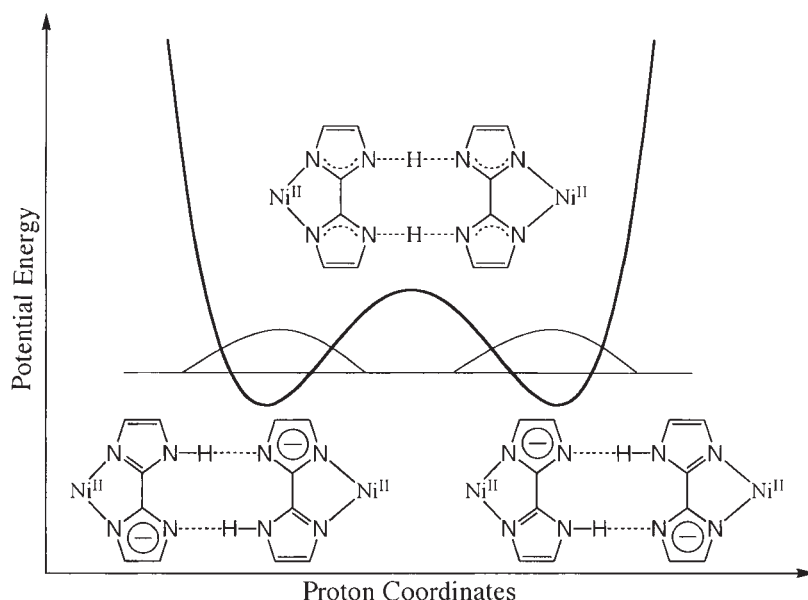


Fig. 2. Schematic view of the double-minimum hydrogen-bond PESs of $[\{\text{Ni}(\text{Hbim})_2\}_n]$ or $(\text{H}_2\text{bim})_n$. The vibrational wave function is also shown.

Table 1. Hydrogen-Bonding Interaction Energies in $(\text{H}_2\text{bim})_n$ and $[\{\text{Ni}(\text{Hbim})_2\}_n]$ Calculated at the B3LYP/CEP-31G(d,p) Level

		<i>n</i>		
		2	3	4
Binding energy/kcal mol ⁻¹	$(\text{H}_2\text{bim})_n$	16.2 (22.5) ^{a)}	15.9	15.8
	$[\{\text{Ni}(\text{Hbim})_2\}_n]$	25.8 (33.6) ^{a)}	23.5	25.8

a) Calculation results at the MP2/CEP-31G(d,p)//B3LYP/CEP-31G(d,p) level.

ing valence orbitals with nodal structures, and is thus suitable to accurately describe the correlation effects of valence electrons. Therefore, to verify the correlation energies given by MP2 calculations using the SBKJC ECPs, we also performed MP2 calculations using our MCPs at the same points. In the MCP calculations, we used Dunning's double zeta basis⁷ for H and the same (d,p) type polarization functions.

The geometry of the $[\text{Ni}^{\text{II}}(\text{Hbim})_2]$ crystal has been found to be a one-dimensional linear structure by an X-ray diffraction experiment.² In such an assembled complex, it has been believed that a cooperative effect plays an important role in obtaining a large binding energy. To verify the existence of cooperative effect in the hydrogen-bond PES, geometry optimizations of $[\{\text{Ni}(\text{Hbim})_2\}_n]$ ($n = 2-4$) were performed. Frequency analyses were performed to confirm that the optimized geometries were stable. The effects of introducing of TMs to hydrogen-bond PES have not yet been well studied. To examine the effect, we also performed geometry optimizations and frequency analyses for $(\text{H}_2\text{bim})_n$, and compared the hydrogen-bonding interaction of $(\text{H}_2\text{bim})_n$ with that of $[\{\text{Ni}(\text{Hbim})_2\}_n]$. The hydrogen-bonding interaction energy per hydrogen-bond pair (binding energy) of $(\text{H}_2\text{bim})_n$ and $[\{\text{Ni}(\text{Hbim})_2\}_n]$ (two N-H...N hydrogen bonds; see Fig. 1) were calculated by the following equations:

$$E_{\text{bind}}[\{\text{Ni}(\text{Hbim})_2\}_n] = \frac{n(E[\{\text{Ni}(\text{Hbim})_2\}_1] - E[\{\text{Ni}(\text{Hbim})_2\}_n])}{n-1}, \quad (1)$$

$$E_{\text{bind}}[(\text{H}_2\text{bim})_n] = \frac{n(E[(\text{H}_2\text{bim})_1] - E[(\text{H}_2\text{bim})_n])}{n-1}. \quad (2)$$

Transition-state optimizations were also performed to obtain the barrier height change between $(\text{H}_2\text{bim})_n$ and $[\{\text{Ni}(\text{Hbim})_2\}_n]$ ($n = 2-4$). Almost all of the calculations were performed in the C_{2h} point group using the Gaussian03 program package⁸ and the MP2 calculations using MCPs were performed by using GAMESS.⁹

Results and Discussion

The calculated binding energies per hydrogen-bond pair of $(\text{H}_2\text{bim})_n$ and $[\{\text{Ni}(\text{Hbim})_2\}_n]$ ($n = 2-4$) are given in Table 1. The calculated hydrogen-bonding interaction energies of $(\text{H}_2\text{bim})_n$ and $[\{\text{Ni}(\text{Hbim})_2\}_n]$ ($n = 2-4$) are approximately 16 kcal mol⁻¹ and 26 kcal mol⁻¹, respectively. The calculated results show that the binding energies of these systems do not depend on the cluster size (n). Thus, a cooperative effect does not appear to play an important role in generating intermolecular hydrogen bonds of H_2bim or $[\text{Ni}(\text{Hbim})_2]$.

Table 2. MP2 Correlation Energies (E_{corr}), Binding Energy (D_e), and Barrier Height (ΔE) in $(\text{H}_2\text{bim})_2$ Calculated with SBKJC and MCP

Energies	SBKJC	MCP
E_{corr} at equilibrium/eV	-73.53	-39.55
E_{corr} at transition state/eV	-74.10	-40.21
E_{corr} at dissociation limit/eV	-72.99	-39.08
Binding energy/kcal mol ⁻¹	22.5	20.1
Barrier height/kcal mol ⁻¹	17.7	15.3

The hydrogen-bonding interaction energies of $[\{\text{Ni}(\text{Hbim})_2\}_n]$ ($n = 2-4$) are approximately 10 kcal mol⁻¹ larger than that of $(\text{H}_2\text{bim})_n$ ($n = 2-4$) at the B3LYP level. The MP2 binding energies of $(\text{H}_2\text{bim})_2$ and $[\{\text{Ni}(\text{Hbim})_2\}_2]$ are 22.5 kcal mol⁻¹ and 33.6 kcal mol⁻¹, respectively. The binding energies of MP2//B3LYP are larger than those of B3LYP by 6 kcal mol⁻¹. At the MP2//B3LYP level, the hydrogen-bonding interaction energies of $[\{\text{Ni}(\text{Hbim})_2\}_n]$ ($n = 2-4$) are also approximately 10 kcal mol⁻¹ larger than that of $(\text{H}_2\text{bim})_n$ ($n = 2-4$). The correlation energies of the MP2 calculations using both SBKJC and MCP are compared in Table 2. Although the correlation energies given by SBKJC are much larger than those by MCP, the correlation energy differences are quite similar to each other. Thus, it is safe to say that the present calculations using the SBKJC ECPs gave results comparable to those by the MCP calculations.

Moreover, the calculated NH vibrational frequency ($\nu(\text{NH})$) is 2852 cm⁻¹ (with no scaling) compared well with the experimental one (2656 cm⁻¹).² These results indicate that the B3LYP calculations used in this study are sufficient to discuss at least the topology of hydrogen-bond PESs.

Why is the hydrogen-bonding interaction of the N-H...N unit strengthened by introducing Ni? What effect does Ni have? In Table 3, the calculated structural parameters of $(\text{H}_2\text{bim})_n$ ($n = 2-4$) and $[\{\text{Ni}(\text{Hbim})_2\}_n]$ ($n = 2-4$) are given. The difference between $(\text{H}_2\text{bim})_n$ ($n = 2-4$) and $[\{\text{Ni}(\text{Hbim})_2\}_n]$ ($n = 2-4$) is the existence of Ni-N coordination bonds. The N(1)-N(6) distance of $[\{\text{Ni}(\text{Hbim})_2\}_n]$ becomes shorter by 0.24-0.35 Å than that of $(\text{H}_2\text{bim})_n$ and the N(2)-N(7) distance longer by 0.14-0.26 Å. These structural changes mean that two imidazole rings of Hbim are slightly distorted from the H_2bim

monomer on the occasion of the formation of Ni-N coordination bonds. Following the distortion of Hbim ligands, the hydrogen bond N-H...N angle is also changed. As shown in Table 3, the N-H...N hydrogen-bond angles of $(\text{H}_2\text{bim})_n$ ($n = 2-4$) and $[\{\text{Ni}(\text{Hbim})_2\}_n]$ ($n = 2-4$) are approximately 162° and 170°, respectively. By introducing Ni, the hydrogen-bond angle becomes 8° more linear. It is well-known that the more linear is a hydrogen bond, the stronger is the hydrogen bond. The linearization of the N-H...N hydrogen bond is one of the reasons why the hydrogen-bonding interaction is strengthened in $[\{\text{Ni}(\text{Hbim})_2\}_2]$ over that in $(\text{H}_2\text{bim})_2$ by 10 kcal mol⁻¹. As a consequence of the existence of the strong hydrogen bond, the H(3)...N(4) intermolecular hydrogen-bond distance of $[\{\text{Ni}(\text{Hbim})_2\}_n]$ ($n = 2-4$) and the N(2)-N(4) distance are 0.13-0.15 Å and 0.10 Å shorter than that of $(\text{H}_2\text{bim})_2$ ($n = 2-4$), respectively.

Finally, we discuss the barrier-height change of the N-H...N hydrogen-bond PES by introducing Ni. At the top (the transition state) of the hydrogen-bond PESs of $(\text{H}_2\text{bim})_2$ and $[\text{Ni}(\text{Hbim})_2]_2$, two vibrations with imaginary frequencies were obtained (second-order transition state: SOTS), respectively. In an N-H...N hydrogen bond, we can generally find an N...H...N proton shared-type transition state (see Fig. 2). $(\text{H}_2\text{bim})_2$ and $[\{\text{Ni}(\text{Hbim})_2\}_2]$ have a pair of two N-H...N hydrogen bonds; it is therefore suitable for our purpose to define the hydrogen-bond PES barrier height as the energy gap between the stable point and SOTS. The PES barrier heights of $(\text{H}_2\text{bim})_2$ and $[\{\text{Ni}(\text{Hbim})_2\}_2]$ are 17.2 kcal mol⁻¹ and 6.3 kcal mol⁻¹ at the B3LYP level and 17.7 kcal mol⁻¹ and 5.2 kcal mol⁻¹ at the MP2//B3LYP level, respectively. Thus, the barrier height of the N-H...N hydrogen-bond PES is drastically decreased by introducing Ni.

The reason why the barrier height is lowered by introducing Ni cannot be simply explained. However, the present results are very important when considering the possibility of creating low barrier hydrogen bond (LBHB), which may play an important role in forming self-assembled structure.¹⁰ In an N-H...N LBHB, the proton is shared equally between two nitrogen atoms and the hydrogen bond is very strong. In other words, the vibrational wave function of the proton motion is delocalized and thus the proton can easily tunnel between two minima of double-minimum hydrogen-bond PESs. To achieve an

Table 3. Important Structural Parameters of Hydrogen-Bond Potentials of $(\text{H}_2\text{bim})_n$ and $[\{\text{Ni}(\text{Hbim})_2\}_n]$ ($n = 2-4$)

		(H ₂ bim) _n			[{Ni(Hbim) ₂ }] _n		
<i>n</i>		2	3	4	2	3	4
Bond length/Å							
	N(2)–H(3)	1.04	1.04	1.04	1.06	1.06	1.06
	H(3)–N(4)	1.87	1.88	1.88	1.74	1.73	1.74
	N(2)–N(4)	2.89	2.89	2.89	2.79	2.79	2.79
	N(1)–N(6)	2.83	2.93	2.93	2.59	2.58	2.59
	N(2)–N(7)	3.12	3.05	3.05	3.26	3.31	3.26
	Ni–N(1)	—	—	—	1.94	1.94	1.94
	Ni–N(6)	—	—	—	1.94	1.94	1.94
Bond angle/deg							
	N(2)–H(3)–N(4)	164.1	161.6	162.1	169.5	172.9	168.6
	N(1)–Ni–N(6)	—	—	—	83.8	83.7	83.8

For $n = 3$ and 4, averaged values are shown. The numbering of atoms is shown in Fig. 1.

LBHB and proton tunneling state, we must control the shape of the double-minimum hydrogen-bond PES, including the height of the PES and the distance between two stable minima.^{11,12} The requirement for delocalizing the proton between two minima of a double-minimum hydrogen-bond PES is achieved if we can make the barrier height low.

As the present study shows, by introducing Ni, the barrier height is lowered and the N...H hydrogen-bond lengths are shortened. The barrier height and the hydrogen-bond length of the formic acid dimer, which exhibit proton tunneling, have been reported to be over 10 kcal mol⁻¹ and ca. 2.7 Å, respectively.¹³ The hydrogen-bond length of [Ni(Hbim)₂] is similar to that of the formic acid dimer (see Table 3) and the barrier height is lower (ca. 6 kcal mol⁻¹). These results imply that proton tunneling occurs in [Ni(Hbim)₂]. Consequently, introduction of TM into the Hbim complex is a good approach to achieving LBHB.

Conclusions

The topologies of the hydrogen-bonding PESs of (H₂bim)_n and [{Ni(Hbim)₂}]_n (*n* = 2–4) were studied by DFT calculations at the B3LYP/CEP-31G(d,p) level. The present results indicate that a cooperative effect does not play an important role in the formation of a one-dimensional assembled structure. The calculated binding energies of [{Ni(Hbim)₂}]_n are 10 kcal mol⁻¹ larger than that of (H₂bim)_n. The hydrogen-bonding interaction is strengthened owing to linearization of the N–H...N intermolecular hydrogen bonds. The N–H...N hydrogen-bond angle of [{Ni(Hbim)₂}]_n (*n* = 2–4) is 8° more linear than that of (H₂bim)_n (*n* = 2–4) on the occasion of the formation of coordination bonds between Hbim and Ni. The calculated results indicate that the barrier height of the hydrogen-bond PES of H₂bim becomes more than 10 kcal mol⁻¹ lower due to the introduction of Ni. Such an effect of a TM suggests that it is capable of controlling the strength of hydrogen-bonding interactions and forming LBHB, which may play an important role to make self-assembled structure. Thus, the combination of hydrogen bonds and coordination bonds is very important for creating self-assembled metal complexes.

References

- 1 M. Tadokoro and K. Nakasuji, *Coord. Chem. Rev.*, **198**, 205 (2000).

- 2 M. Tadokoro, H. Kanno, T. Kitajima, H. Shimada-Umemoto, N. Nakanishi, K. Isobe, and K. Nakasuji, *Proc. Natl. Acad. Sci. U.S.A.*, **99**, 4950 (2002).
- 3 W. J. Stevens, H. Basch, and M. Krauss, *J. Chem. Phys.*, **81**, 6026 (1984).
- 4 W. J. Stevens, M. Krauss, H. Basch, and P. G. Jasien, *Can. J. Chem.*, **70**, 612 (1992).
- 5 T. Noro, M. Sekiya, Y. Osanai, E. Miyoshi, and T. Koga, *J. Chem. Phys.*, **119**, 7693 (2003).
- 6 Y. Sakai, E. Miyoshi, M. Klobukowski, and S. Huginaga, *J. Chem. Phys.*, **106**, 8084 (1997).
- 7 T. H. Dunning, Jr., *J. Chem. Phys.*, **53**, 2823 (1970).
- 8 M. J. Frisch, G. W. Trucks, H. B. Schlegel, G. E. Scuseria, M. A. Robb, J. R. Cheeseman, J. A. Montgomery, Jr., T. Vreven, K. N. Kudin, J. C. Burant, J. M. Millam, S. S. Iyengar, J. Tomasi, V. Barone, B. Mennucci, M. Cossi, G. Scalmani, N. Rega, G. A. Petersson, H. Nakatsuji, M. Hada, M. Ehara, K. Toyota, R. Fukuda, J. Hasegawa, M. Ishida, T. Nakajima, Y. Honda, O. Kitao, H. Nakai, M. Klene, X. Li, J. E. Knox, H. P. Hratchian, J. B. Cross, C. Adamo, J. Jaramillo, R. Gomperts, R. E. Stratmann, O. Yazyev, A. J. Austin, R. Cammi, C. Pomelli, J. W. Ochterski, P. Y. Ayala, K. Morokuma, G. A. Voth, P. Salvador, J. J. Dannenberg, V. G. Zakrzewski, S. Dapprich, A. D. Daniels, M. C. Strain, O. Farkas, D. K. Malick, A. D. Rabuck, K. Raghavachari, J. B. Foresman, J. V. Ortiz, Q. Cui, A. G. Baboul, S. Clifford, J. Cioslowski, B. B. Stefanov, G. Liu, A. Liashenko, P. Piskorz, I. Komaromi, R. L. Martin, D. J. Fox, T. Keith, M. A. Al-Laham, C. Y. Peng, A. Nanayakkara, M. Challacombe, P. M. W. Gill, B. Johnson, W. Chen, M. W. Wong, C. Gonzalez, and J. A. Pople, "Gaussian 03" Gaussian, Inc., Pittsburgh PA (2003).
- 9 M. W. Schmidt, K. K. Baldridge, J. A. Boatz, S. T. Elbert, M. S. Gordon, J. J. Jensen, S. Koseki, N. Matsunaga, K. A. Nguyen, S. Su, T. L. Windus, M. Dupuis, and J. A. Montgomery, *J. Comput. Chem.*, **14**, 1347 (1993).
- 10 K. S. Kim, S. B. Suh, J. C. Kim, B. H. Hong, E. C. Lee, S. Yun, P. Tarakeshwar, J. Y. Lee, Y. Kim, H. Ihm, H. G. Kim, J. W. Lee, J. K. Kim, H. M. Lee, D. Kim, C. Cui, S. J. Youn, H. Y. Chung, H. S. Choi, C. Lee, S. J. Cho, S. Jeong, and J. Cho, *J. Am. Chem. Soc.*, **124**, 14268 (2002).
- 11 H. Mori, H. Sekiya, E. Miyoshi, K. Mogi, and Y. Sakai, *J. Chem. Phys.*, **119**, 4159 (2003).
- 12 H. Mori, J. Furusawa, and H. Sekiya, *Bull. Pol. Acad. Sci.*, **50**, 451 (2002).
- 13 N. Shida, P. F. Barbara, and J. Almlöf, *J. Chem. Phys.*, **94**, 3633 (1991).